J. Ocean Univ. China (Oceanic and Coastal Sea Research)
https://doi.org/10.1007/s11802-023-5570-0
ISSN 1672-5182, 2023 22 (5): 1353-1360
http://www.ouc.edu.cn/xbywb/
E-mail:xbywb@ouc.edu.cn

Density Functional Theory Study of Marine Polybrominated Diphenyl Ethers in Anaerobic Degradation

XU Xiang1), *, MAN Miaomiao1), SUN Qinxing1), LIU Qingzhi1), WU Kechen2), and YANG Dengfeng1)

1) *College of Chemistry and Pharmaceutical Sciences*, *Qingdao Agricultural University*, *Qingdao* 266109, *China*
2) *Fujian Key Laboratory of Functional Marine Sensing Materials*, *Minjiang University*, *Fuzhou* 350108, *China*

(Received October 21, 2022; revised December 10, 2022; accepted February 20, 2023)

Abstract Polybrominated diphenyl ethers (PBDEs) are a kind of serious pollutants in the ocean. Biodegradation is considered as an economical and safe way for PBDEs removal and reductive debromination dominates the initial pathway of anaerobic degradation. On the basis of experimental study, Octa-BDE 197, Hepta-BDE 183, Hexa-BDE 153, Penta-BDE 99 and Tetra-BDE 47 were selected as the initial degradation objects, and their debromination degradation were studied using density functional theory. The structures were optimized by Gaussian 09 program. Furthermore, the molecular orbitals and charge distribution were analyzed. All C-Br bond dissociation energies at different positions including ortho, meta and para bromine atoms were calculated and the sequence of debromination was obtained. There is a close relationship between molecular structure, charge, molecular orbital and C-Br bond. All PBDEs exhibited similar debromination pathways with preferential removal of meta and para bromines.

Key words polybrominated diphenyl ethers; reductive debromination; anaerobic degradation; density functional theory; bond dissociation energies

1 Introduction

Polybrominated diphenyl ethers (PBDEs) are a kind of global organic pollutants widely existing in marine environment (Wang *et al*., 2011; Patrik *et al*., 2022). Water is an important medium for the migration and diffusion of PBDEs. When they enterthe ocean from the sea surface, some volatile gases enter the air, causing air pollution; the others migrate with the current, some of which are absorbed by sediments, and some of which are absorbed by aquatic animals and plants to cause biological enrichment, and then enters higher organisms and even human bodies along the food chain. PBDEs have attracted great attention due to its biotoxicity, such as endocrine disruption effect to mammalian tissues (Song *et al*., 2015; Zhu, *et al*., 2017).

PBDEs in the environment are stable in the environment because of their long half-life, so they are not easy to be degraded. Therefore, the method of human intervention to degrade PBDEs plays important role in environmental protection (Chen *et al*., 2017). At present, the main degradation methods of PBDEs include biodegradation (Chen *et al*., 2016; Ming *et al*., 2017), photolysis (Bezares *et al*., 2004; Eriksson *et al*., 2006), zerovalent iron reduction (Keum *et al*., 2005) and so on. Biodegradation is considered as an economical and safe way for PBDEs removal (Zhao *et al*., 2018).

The biodegradation of PBDEs mainly includes aerobic bacteria and anaerobic bacteria. The aerobic degradation pathways of PBDEs include cleavage of aromatic ring, debromination, and hydroxylation, while reductive debromination dominates the initial pathway of anaerobic degradation (Zhao *et al*., 2018). PBDEs can be debrominated under anaerobic conditions by dehalogenating bacteria (Gerecke *et al*., 2005; Qiu e*t al*., 2012). Lee *et al*. (2010) carried out a series of studies on high brominated polybrominated diphenyl ethers in seawater sediments. After 60 days of degradation by anaerobic bacteria, a variety of low brominated diphenyl ethers were detected in the products. When Robrock *et al*. (2008) studied the degradation of the same high brominated PBDEs, they also found that all substrates underwent reductive debromination reaction and were converted into diphenyl ethers with lower bromine content. Gerecke *et al*. (2005) found that BDE-208 and BDE-207 were the first to be degraded in the degradation products when anaerobic bacteria degraded polybrominated diphenyl ethers, while BDE-206 was not generated at the same time.

With the development of theoretical chemistry and computer technology, computational chemistry has been

---

* Corresponding author. Tel: 0086-532-58957895
E-mail: rainerxu@163.com

applied more and more to the research of environmental pollution (Altarawneh *et al*., 2020; Xu *et al*., 2021; Mateusz *et al*., 2022). On the one hand, the theoretical research results can verify and illustrate the experimental results; on the other hand, they can provide the microscopic theoretical results such as charge, molecular orbitals and intermediates that cannot be detected in the experiment. In the theoretical study of PBDEs, Shi *et al.* (2015) studied the oxidative degradation of decabromodiphenyl ether (BDE 209) using DFT. Luo *et al.* (2015) studied on the excited states and photodebromination of 20 selected polybrominateddiphenyl ether congeners involving a π–σ* excitation using DFT and time-dependent DFT (TD-DFT).

In this paper, on the basis of the experimental study (Robrock *et al*., 2008) about the anaerobic degradation process of PBDEs, the density functional theory and Gaussian 09 software package are useded. Octa-BDE 197(2,2',3,3',4,4',6,6'-octabromodiphenyl ether), Hepta-BDE 183(2,2',3,4,4',5',6-Heptabromodiphenyl ether), Hexa-BDE 153(2,2',4,4',5,5'-Hexabromodiphenyl ether), Penta-BDE 99(2,2',4,4',5-Pentabromodiphenyl ether) and Tetra-BDE 47(2,2',4,4'-tetrabromodiphenyl ether) were selected as the initial degradation objects. These representatives are chosen because they represent the polybrominated diphenyl ethers with different number of brominated substituents. The study of their degradation shows the law of the progressive degradation of polybrominated diphenyl ethers. The structure of them and their debrominated products were optimized to obtain the optimal structures with the lowest energy. In order to better understand the reaction of reductive debromination, the bond length, bond angle, molecular orbital and charge distribution of five PBDEs were analyzed, and the bond dissociation energies of all C-Br bonds were calculated.

2 Calculation Methods

DFT calculations have been carried out using the B3LYP (Lee *et al*., 1988; Axel, 1998) exchange correlation functionals with 6-31+G(d) basis set. Solvent effects have been considered using a selfconsistent reaction field (SCRF) (Simkin *et al*., 1994) based on the polarizable continuum model (PCM) of the Tomasi's group (Barone *et al*., 1998). The optimized structures were analyzed by natural bond orbital (NBO) method (Reed *et al*., 1988). All calculations were carried out with the Gaussian 09 program (Frisch *et al*., 2010). All the molecular structures were created by GaussView soft. Then the Gaussian software was used to optimize the structure, calculate the frequency, analyze the natural bond orbital and calculate the energy. Finally, GaussView was used to view graphics, such as optimized structures, infrared spectra, and molecular orbitals.

3 Results and Discussion

3.1 Optimized Structures of Five Selected PBDEs

The optimized structures of Octa-BDE 197, Hepta-BDE 183, Hexa-BDE 153, Penta-BDE 99 and Tetra-BDE 47 are shown in Fig.1. Frequency calculation was performed to ensure that the molecules were at the minimal potential energy surface. All optimized molecular structures have no virtual frequency.

Fig.1 shows that the main structures of the five PBDEs

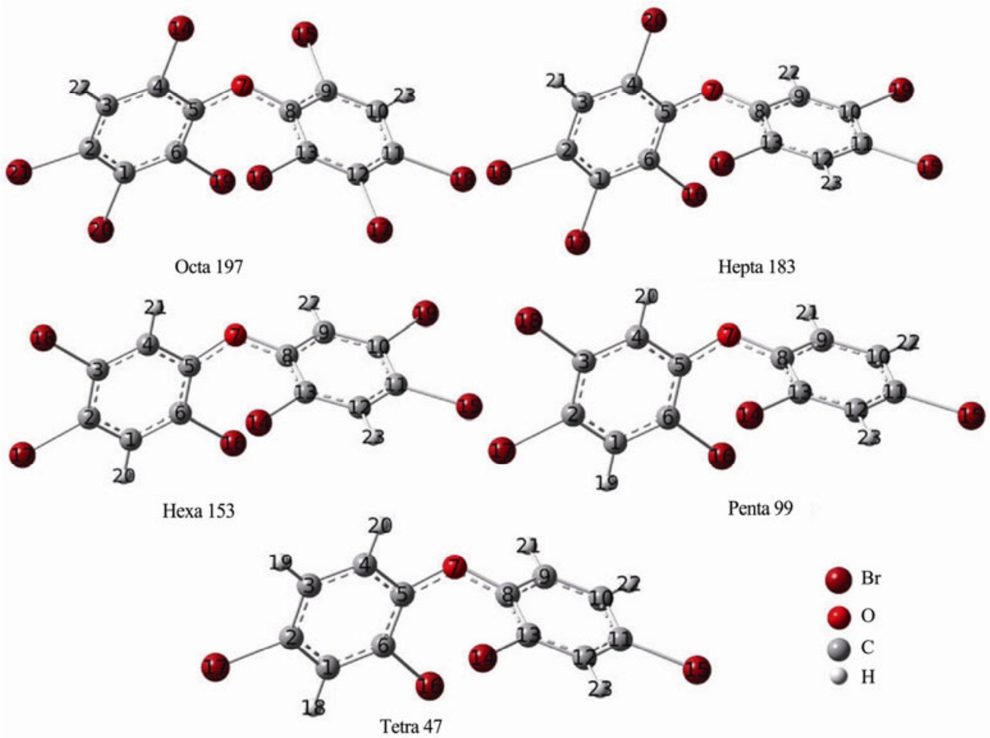

Fig.1 Optimized structure of Octa-BDE 197, Hepta-BDE 183, Hexa-BDE 153, Penta-BDE 99 and Tetra-BDE 47. The atomic numbers in the figure are randomly generated by the computing software.

are approximately similar. The C-Br bond and the benzene ring are almost in the same plane, and the two benzene rings are staggered at a certain angle to reduce steric hindrance. The O atom is almost coplanar with the two benzene rings, and the dihedral angles C4-C5-C6-O7 and C9-C8-C13-O7 between the two benzene rings and the O atom are about 174°. Meanwhile, the dihedral angle C6-C5-O7-C8 is −48° (except Hepta 183 is −65°), indicating that the planes of the two benzene rings are staggered and not in the same plane. PBDEs with different amounts of bromine atoms have slight differences in bond angles, such as the angle range of C5-O7-C8 is about 124–126°, and the angle range of C4-C5-C6 is about 119–120°. It can be inferred that bromine atoms have little influence on the main structure of PBDEs.

By comparing the bond lengths of two ether bonds in the same PBDEs molecule, it can be found that if the bromine substitutions of benzene rings on both sides are exactly the same, the ether bond lengths are basically the same. If bromine substitutions in the benzene ring are different, the ether bond lengths are different. For example, the ether bond lengths of C5-O7 and C8-O7 in Octa197 are both 1.3687 Å, while the ether bond lengths of C5-O7 and C8-O7 in Hepta 183 are 1.3704 and 1.3789 Å, respectively. For different PBDEs molecules, ether bonds at the same position have different bond lengths due to different bromine substitutions. For example, the bond length of C8-O7 is 1.3687 Å in Octa 197, while it is 1.3807 Å in Penta 99, indicating that different amounts of bromine atoms have certain effect on the bond length of ether bonds. The C-Br bond length is about 1.90 Å, which is consistent with the results of literature studies (Wang *et al.*, 2015).

3.2 Natural Population Analysis (NPA) Charges Analysis

By natural bond orbital analysis, the electronic structures of stationary points were analyzed and the NPA charges of 5 PBDEs were got. The NPA charges are shown in Table 1.

Table 1 NPA charges of each atom in Octa 197, Hepta 183, Hexa 153, Penta 99 and Tetra 47

Octa 197	NPA charges	Hepta 183	NPA charges	Hexa 153	NPA charges	Penta 99	NPA charges	Tetra 47	NPA charges
C1	−0.1630	C1	−0.1657	C1	−0.2315	C1	−0.2321	C1	−0.2495
C2	−0.1379	C2	−0.1340	C2	−0.1521	C2	−0.1533	C2	−0.1318
C3	−0.2326	C3	−0.2348	C3	−0.1406	C3	−0.1407	C3	−0.2366
C4	−0.1379	C4	−0.1344	C4	−0.2450	C4	−0.2460	C4	−0.2354
C5	0.2833	C5	0.2751	C5	0.2981	C5	0.3004	C5	0.2830
C6	−0.1709	C6	−0.1624	C6	−0.1653	C6	−0.1654	C6	−0.1627
O7	−0.5037	O7	−0.5096	O7	−0.5138	O7	−0.5164	O7	−0.5196
C8	0.2833	C8	0.3047	C8	0.2981	C8	0.2806	C8	0.2830
C9	−0.1379	C9	−0.2486	C9	−0.2450	C9	−0.2345	C9	−0.2354
C10	−0.2326	C10	−0.1381	C10	−0.1406	C10	−0.2359	C10	−0.2366
C11	−0.1379	C11	−0.1548	C11	−0.1521	C11	−0.1308	C11	−0.1318
C12	−0.1630	C12	−0.2291	C12	−0.2315	C12	−0.2489	C12	−0.2495
C13	−0.1709	C13	−0.1725	C13	−0.1653	C13	−0.1627	C13	−0.1627
Br14	0.1183	Br14	0.1068	Br14	0.1070	Br14	0.0966	Br14	0.0947
Br15	0.1183	Br15	0.1043	Br15	0.1045	Br15	0.0698	Br15	0.0684
Br16	0.1446	Br16	0.1433	Br16	0.1070	Br16	0.1055	Br16	0.0947
Br17	0.1421	Br17	0.1420	Br17	0.1045	Br17	0.1033	Br17	0.0684
Br18	0.1162	Br18	0.1177	Br18	0.1089	Br18	0.1074	H18	0.2812
Br19	0.1446	Br19	0.1094	Br19	0.1089	H19	0.2862	H19	0.2739
Br20	0.1421	Br20	0.1177	H20	0.2867	H20	0.2855	H20	0.2746
Br21	0.1162	H21	0.2895	H21	0.2862	H21	0.2753	H21	0.2746
H22	0.2895	H22	0.2868	H22	0.2862	H22	0.2744	H22	0.2739
H23	0.2895	H23	0.2867	H23	0.2867	H23	0.2817	H23	0.2812

According to the data in Table 1, the natural charges of bromine and hydrogen atoms are all positive values. In the benzene ring, all the C atoms except C5 and C8 have negative natural charges, and all the oxygen atoms have positive natural charges. According to its structure, it can be inferred that the electron absorption of oxygen atom causes the charge transfer of carbon atoms connected with oxygen atom, and the electrons are transferred from carbon atoms to oxygen atom, so that the carbon atom has positive charge. Because Octa197, Hexa 153 and Tetra 47 have symmetric structures, the natural charges of C5 and C8 are similar, while the natural charges of C5 and C8 in Hepta 183 and Penta 99 are different.

In addition, from the data in each row of the table from left to right, that is, with the gradual decrease of the number of bromine substituents, it can be found that the negative charges of C1, C9 and O7 increase while the positive charges of bromine decrease. This means that the more bromine there is, the less negative charge C1, C9, and O7 will have, so bromine has an electron absorption effect.

3.3 Molecular Frontier Orbital Analysis

Frontier orbital theory (Fukui *et al.*, 1952) is to divide the electron cloud around the molecule into multiple molecular orbitals of different energy levels according to the energy. According to the theory, the highest occupied molecular orbital (HOMO) and lowest unoccupied molecular orbital (LUMO) are key to determining how a chemical reaction will take place in a system. When oxidation reaction occurs, the lower the energy of LUMO orbital, the easier it is to be filled by electrons, and the stronger the oxidation ability; similarly, the higher the HOMO, the more likely it is to lose electrons, and the more reductive it is. The HOMO and LUMO of Octa-BDE 197, Hepta-BDE 183, Hexa-BDE 153, Penta-BDE 99 and Tetra-BDE 47 are shown in Fig.2.

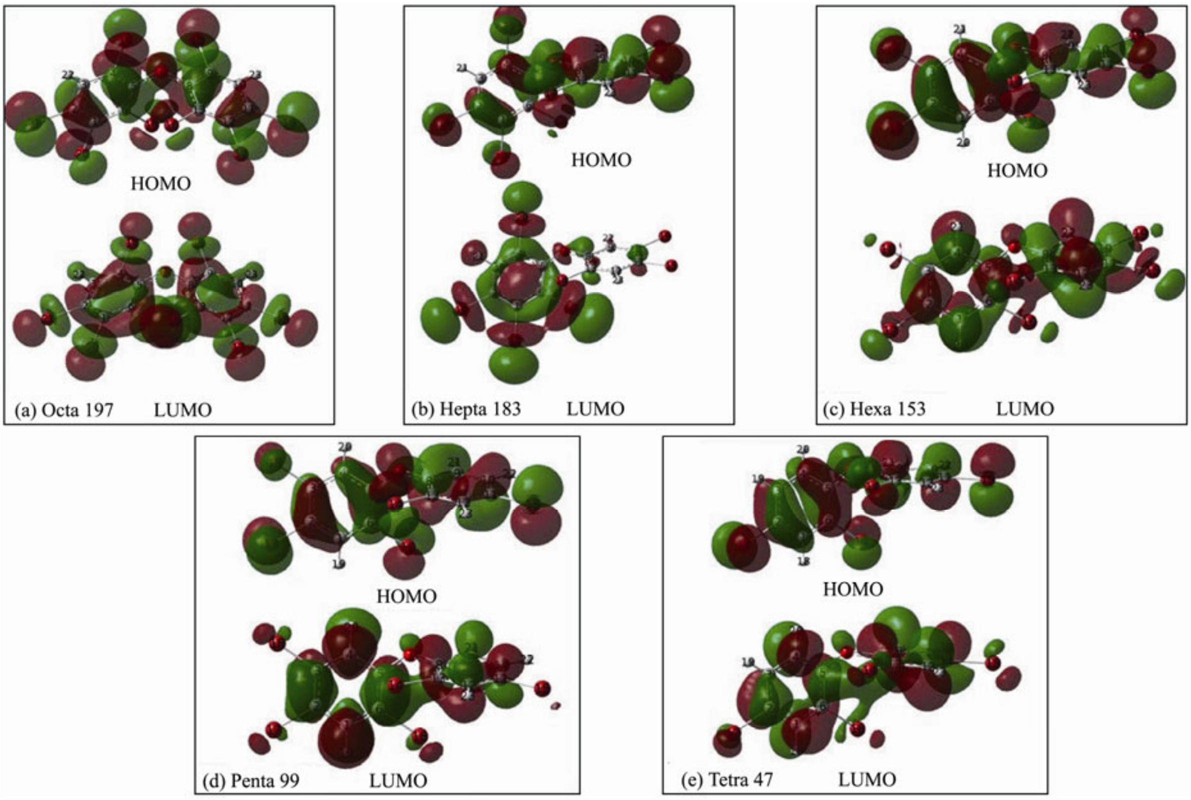

Fig.2 The HOMO and LUMO of (a) Octa-BDE 197, (b) Hepta-BDE 183, (c) Hexa-BDE 153, (d) Penta-BDE 99 and (e) Tetra-BDE 47. The red area is the positive phase, and the green area is the negative phase.

According to the calculation results, the HOMO energies of Octa-BDE 197, Hepta-BDE 183, Hexa-BDE 153, Penta-BDE 99 and Tetra-BDE 47 are −0.25096, −0.24994, −0.24766, −0.24489 and −0.24222 Hartree, respectively. As the number of bromine atoms decreases, the HOMO energy increases gradually, so it can be judged that the reductive debromination reaction of anaerobic bacteria becomes easier. This result is consistent with previous research (Zhao *et al*., 2015).

Fig.2 shows the frontier molecular orbitals of five PBDEs. Because the molecular structure of octa-BDE 197 is symmetric, the distribution of the electron clouds of HOMO and LUMO orbitals is uniform. Where LUMO has the σ* character, while HOMO has π character, and C-Br bond electron cloud is plump. Hepta-BDE 183 differs from that for its HOMO preferres to spread mainly over the aromatic ring of fewer bromine substituents. The LUMO is mainly located on the phenyl group which has relatively more bromine substituents (Luo *et al*., 2015). With the reduction of bromine substituents, the electron cloud density of Hexa-BDE 153, Penta-BDE 99 and Tetra-BDE 47 can be seen to decrease gradually, especially for the LUMO orbitals. This is also consistent with the results of the charge analysis in the previous part. Because different brominations lead to different structures, and the different structures lead to different electron clouds, which leads to different strength of chemical bonds, and further leads to the difference in reductive debromination.

3.4 Bond Dissociation Energies Analysis

The bond dissociation energy is also referred to as bond energy, binding energy, bond strength, or bond disruption energy (Luo, 2007), which can be used to determine the strength of a chemical bond or the difficulty of breaking it. For instance, during the hydrodeoxygenation process, Prasomsri *et al*. (2014) got the bond strengths order of Ph-OH > Ph-OMe > Ph-O-Ph > Ph-O-Me by the bond dissociation energy analysis of phenolic C-O bonds. In this paper, by comparing the C-Br bond dissociation energies at different position of PBDEs, the order of reductive debromination can be inferred. The C-Br bond with smaller bond dissociation energies is easier to break, while the C-Br bond with larger bond dissociation energies is more difficult. The energy of the two radical molecular fragments formed after the break minus the energy of the reactant is the bond dissociation energies, which is shown as follows:

$$E_{\text{C-Br}} = E_{\text{BDE-radical}} + E_{\text{Br-radical}} - E_{\text{BDE}} .$$

All possible debromination paths of 5 PBDEs are shown in Fig.3, where the solid arrows represent the debromination of products detected in the experiment and the dashed lines are other possible debromination ways. The dots in the molecular formula represent the position of debromination. We hope to study all possible debromination pathways, discuss the existing experimental results through comparison and verification with experiments (Gerecke *et al.*, 2005; Robrock *et al.*, 2008; Tokarz Iii *et al.*, 2008; Ding *et al.*, 2013; Huang *et al.*, 2014) and analyze the possible reasons why some products cannot be detected.

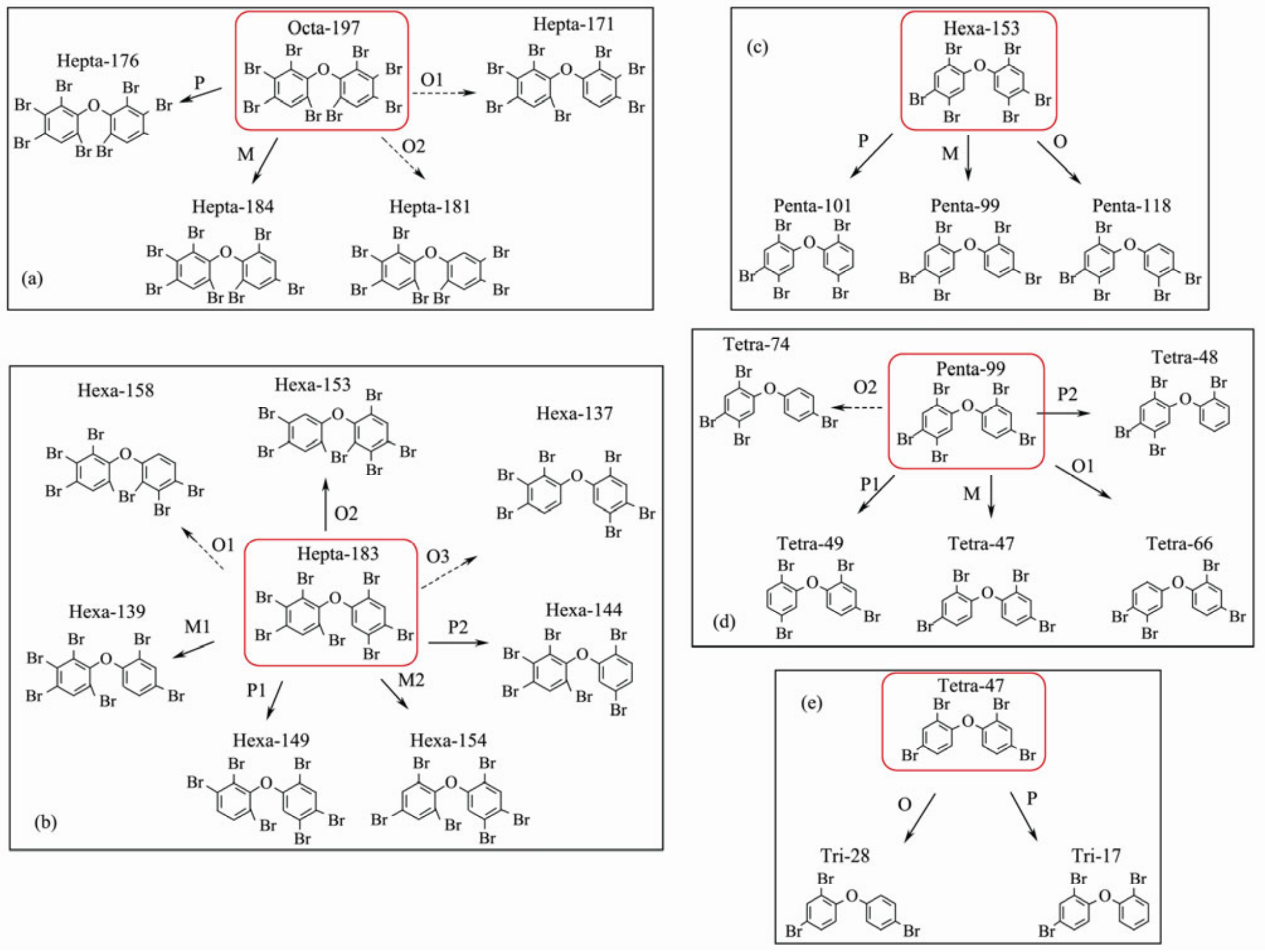

Fig.3 The possible debromination paths of 5 PBDEs (a) Octa-BDE 197, (b) Hepta-BDE 183, (c) Hexa-BDE 153, (d) Penta-BDE 99 and (e) Tetra-BDE 47. O, ortho debromination; M, meta debromination; P, para debromination.

The calculated results of all the C-Br bond dissociation energies of 5 PBDEs are listed in Table 2. There are four types of C-Br bond in Octa-BDE 197, namely P, M, O1 and O2, and the bond dissociation energies are in the order of M < P < O2 < O1. The bond dissociation energy of the C-Br bond in meta-position is the smallest, which is 362.36 kJ mol^{-1}. Under the same conditions of anaerobic bacteria, the bond is the easiest to break, so meta debromination is the most preferred and the product Hepta-184 can be obtained. The second is para debromination with the C-Br bond dissociation energies of 363.42 kJ mol^{-1} and the product is Hepta-176. The orth debromination is the most difficult, and the two products Hepta-171 and Hepta-181 were not detected in the experiment (Robrock *et al.*, 2008). Hepta-183 has more debromination modes and the debromination rule was found to be the same as that of Octa-197. The ortho debromination was the most difficult, and only one ortho debromination product Hexa-153 was detected in the experiment. According to the data in Table 2, Hexa-153, Penta-99 and Tetra-47 with less bromine substitutions also have similar debromination laws just as Octa-197. In summary, it can be found that the products which are not detected in the experiment are those with higher bond dissociation energy. This is because the larger the bond dissociation energy, the more difficult it is to break.

Of course, not all ortho debromination was undetectable, and some ortho debromination also was detected in the experiment. The experimental results (Kristin *et al.*, 2008) showed that the ortho substituted products were usually minor and sometimes not even produced when compared with the para and meta bromine removal products. In the case of polychlorinated biphenyls and polybrominated biphenyls, it was also found that the removal of ortho halogens was the most difficult (Hartkamp-Commandeur *et al.*, 1996; Morris, 1999; Bedard *et al.*, 2000). Among ortho, meta and para debromination, meta and para debromination are preferred. In Octa-197, Hepta-183, Hexa-153 and Penta-99, meta and para debromination are found in Table 2. Except Hexa-153, the other molecules are meta C-Br bond with smaller bond dissociation energies, and meta debromination are more preferred than para debromination.

Table 2 All the C-Br bond energy of 5 PBDEs (a) Octa-BDE 197, (b) Hepta-BDE 183, (c) Hexa-BDE 153, (d) Penta-BDE 99 and (e) Tetra-BDE 47

PBDEs	Debromination position	E_{BDE}, $E_{\mathrm{BDE\text{-}radical}}$ /Hartree	$E_{\mathrm{C\text{-}Br}}$/kJ/mol	Sequence list
Octa-197	-	−21107.54492	-	
Hepta-176	P	−18535.72623	363.42	M < P < O2 < O1
Hepta-184	M	−18535.72666	362.36	
Hepta-171	O1	−18535.72166	374.83	
Hepta-181	O2	−18535.72467	367.32	
Hepta-183	-	−18536.42058	-	
Hexa-139	M1	−15964.60174	363.80	M2 < M1 < P2 < P1 < O1 < O2 <O3
Hexa-149	P1	−15964.60160	364.15	
Hexa-154	M2	−15964.60240	362.16	
Hexa-144	P2	−15964.60173	363.82	
Hexa-153	O2	−15964.60030	369.36	
Hexa-158	O1	−15964.59951	367.40	
Hexa-137	O3	−15964.59649	376.89	
Hexa-153	-	−15965.29484	-	
Penta-101	P	−13393.47626	363.16	P < M < O
Penta-118	O	−13393.47479	366.83	
Penta-99	M	−13393.47617	363.39	
Penta-99	-	−13394.16973	-	
Tetra-49	P1	−10822.35131	362.77	M < P1 < P2 < O1 < O2
Tetra-48	P2	−10822.35122	362.98	
Tetra-66	O1	−10822.34987	366.34	
Tetra-40	M	−10822.35143	367.03	
Tetra-74	O2	−10822.34960	362.46	
Tetra-47	-	−10823.04497	-	
Tri-28	O	−8251.22465	367.49	P < O
Tri-17	P	−8251.22638	363.19	

Notes: Calculated energy correction factor is 0.95. The bold characters in the table are debrominated products that were not detected in the experiment. O, ortho-debromination; M, meta-debromination; P, para-debromination.

4 Conclusions

In this study, Octa-BDE 197, Hepta-BDE 183, Hexa-BDE 153, Penta-BDE 99 and Tetra-BDE 47 were selected as the initial degradation objects, and their debromination degradation were studied at B3LYP/6-31+G(d) level.

According to the optimized structures of five selected PBDEs, the C-Br bond and the benzene ring are almost in the same plane, and the two benzene rings are staggered at a certain angle to reduce steric hindrance. Different amounts of bromine atoms have certain effect on the bond length of ether bonds. By natural bond orbital analysis, the electronic structures of stationary points were analyzed. The more bromine there is, the less negative charge C1, C9, and O7 will have, so bromine will have an electron sucking effect. By molecular frontier orbital analysis, it can be got that as the number of bromine atoms decreases, the reductive debromination reaction of anaerobic bacteria becomes easier. By comparing the C-Br bond dissociation energies at different positions, all PBDEs exhibited similar debromination pathways with preferential removal of para and meta bromines. The results can provide a theoretical basis for the anaerobic debromination and degradation of PBDEs, and also provide a theoretical guidance for the removal of PBDEs from Marine pollutants.

Acknowledgements

This study is financially supported by the National Natural Science Foundation of China (Nos. 41406090, 42176045), the Science Foundation of Qingdao Agricultural University (No. 631302), the Fujian Key Laboratory of Functional Marine Sensing Materials, Minjiang University (No. MJUKF-FMSM202102), and the Natural Science Foundation of Shandong Province (Nos. ZR2019 MB020, ZR2020MB119).

References

Altarawneh, M., Saeed, A., Siddique, K., Jansson, S., and Dlugogorski, B. Z., 2020. Formation of polybrominated dibenzofurans (PBDFs) and polybrominated diphenyl ethers (PBDEs) from oxidation of brominated flame retardants (BFRs). *Journal of Hazardous Materials*, **400**: 123166.

Axel, B. D., 1998. Density-functional thermochemistry. III. The role of exact exchange. *Journal of Chemical Physics*, **98**: 5648-5652.

Barone, V., And, M. C., and Tomasi, J., 1998. Geometry optimization of molecular structures in solution by the polarizable continuum model. *Journal of Computational Chemistry*, **19**: 404-417.

Bedard, D. L., and Van Dort, H. M., 1998. Complete reductive dehalogenation of brominated biphenyls by anaerobic microorganisms in sediment. *Applied and Environmental Microbiology*, **64** (3): 940-947.

Bezares-Cruz, J., Jafvert, C. T., and Hua, I., 2004. Solar photodecomposition of decabromodiphenyl ether: products and quantum yield. *Environmental Science & Technology*, **38**: 4149-4156.

Chen, F., Yang, Q., Wang, S., Yao, F., Sun, J., Wang, Y., *et al*., 2017. Graphene oxide and carbon nitride nanosheets co-modified silver chromate nanoparticles with enhanced visible-light photoactivity and anti-photocorrosion properties towards multiple refractory pollutants degradation. *Applied Catalysis B-Environmental*, **209**: 493-505.

Chen, M., Qin, X., and Zeng, G., 2016. Single-walled carbon nanotube release affects themicrobial enzyme-catalyzed oxidation processes of organic pollutants and lignin model compounds in nature. *Chemosphere*, **163**: 217-226.

Ding, C., Chow, W. L., and He, J., 2013. Isolation of Acetobacterium sp. strain AG, which reductively debrominates octa- and pentabrominated diphenyl ether technical mixtures. *Applied and Environmental Microbiology*, **79** (4): 1110-1117.

Eriksson, J., Green, N., Marsh, G., and Bergman, A., 2004. Photochemical decomposition of 15 polybrominated diphenyl ether congeners in methanol/water. *Environmental Science & technology*, **38**: 3119-3125.

Frisch, M. J., Trucks, G. W., Schlegel, H. B., Scuseria, G. E., Robb, M. A., Cheeseman, J. R., *et al*., 2010. *Gaussian 09*, Revision B.01.

Fukui, K., and Yonezawa, T., 1952. A molecular orbital theory of reactivity in aromatic hydrocarbons. *Journal of Chemical Physics*, **20**: 722-726.

Gerecke, A. C., Hartmann, P. C., Heeb, N. V., Kohler, H. P., Giger, W., Schmid, P., *et al*., 2005. Anaerobic degradation of decabromodiphenyl ether. *Environmental Science & Technology*, **39** (4): 1078-1083.

Hartkamp-Commandeur, L. C. M., Gerritse, J., Govers, H. A. J., and Parsons, J. R., 1996. Reductive dehalogenation of polychlorinated biphenyls by anaerobic microorganisms enriched from dutch sediments. *Chemosphere*, **32** (7): 1275-1286.

Huang, H. W., Chang, B. V., and Lee, C. C., 2014. Reductive debromination of decabromodiphenyl ether by anaerobic microbes from river sediment. *International Biodeterioration and Biodegradation*, **87**: 60-65.

Keum, Y. S., and Li, Q. X., 2005. Reductive debromination of polybrominated diphenyl ethers by zerovalent iron. *Environmental Science & Technology*, **39**: 2280-2286.

Lee, C., Yang, W., and Parr, R. G., 1988. Development of the Colle-Salvetti correlation-energy into a functional of the electron density. *Physical Review B*, **37**: 785-789.

Lee, L. K., and He, J., 2010. Reductive debromination of polybrominated diphenyl ethers by anaerobic bacteria from soils and sediments. *Applied and Environmental Microbiology*, **76** (3): 794-802.

Lee, L. K., Ding, C., Yang, K. L., and He, J., 2011. Complete debromination of tetra- and penta-brominated diphenyl ethers by a coculture consisting of dehalococcoides and desulfovibrio species. *Environmental Science & Technology*, **45**: 8475-8482.

Luo, J., Hu, J., Wei, X., Li, L., and Huang, X., 2015. Excited states and photodebromination of selected polybrominated diphenyl ethers: Computational and quantitative structure-property relationship studies. *International Journal of Molecular Sciences*, **16** (1): 1160-1178.

Luo, Y. R., 2007. *Comprehensive Handbook of Chemical Bond Energies*. CRC Press, 1233-1240.

Mateusz, P., Timo, R., Frederik, R. W., Agata, P., and Piotr, P., 2022. Environment-friendly transesterification to seawater-degradable polymers expanded: Computational construction guide to breaking points. *Chemosphere*, **308**, Part 2: 136381.

Ming, C., Zeng, G., Cui, L., Chang, Z., Xu, P., Min, Y., *et al*., 2017. Interactions of carbon nanotubes and/or graphene with manganese peroxidase during biodegradation of endocrine disruptors and triclosan. *Chemosphere*, **184**: 127-136.

Morris, P., Quensen, J. F., Tiedje, J. M., and Boyd, S. A., 1992. Reductive debromination of the commercial polybrominated biphenyl mixture firemaster BP6 by aerobic microorganisms from sediments. *Applied and Environmental Microbiology*, **58** (10): 3249-3256.

Patrik, F., Katrin, V., and Jakob, S., 2022. Residual additives in marine microplastics and their risk assessment – A critical review, *Marine Pollution Bulletin*, **177**: 113467.

Prasomsri, T., Shetty, M., Murugappana, K., and Román-Leshkov, Y., 2014. Insights into the catalytic activity and surface modification of MoO_3 during the hydrodeoxygenation of lignin-derived model compounds into aromatic hydrocarbons under low hydrogen pressures. *Energy & Environmental Science*, **7**: 2660-2669.

Qiu, M., Chen, X., and Deng, D., 2012. Effects of electron donors on anaerobic microbial debromination of polybrominated diphenyl ethers (PBDEs). *Biodegradation*, **23**: 351-361.

Reed, A. E., Curtiss, L. A., and Weinhold, F., 1988. Intermolecular interactions from a natural bond orbital, donor-acceptor viewpoint. *Chemical Reviews*, **88**: 899-926.

Robrock, K. R., Korytar, P., and Alvarez-Cohen, L., 2008. Pathways for the anaerobic microbial debromination of polybrominated diphenyl ethers. *Environmental Science & Technology*, **42** (8): 2845-2852.

Shi, J., Qu, R., Feng, M., Wang, X., Wang, L., Yang, S., *et al*., 2015. Oxidative degradation of decabromodiphenyl ether (BDE 209) by potassium permanganate: Reaction pathways, kinetics, and mechanisms assisted by density functional theory calculations. *Environmental Science & Technology*, **49** (7): 4209-4217.

Simkin, B. I., Sheikhet, I. I., and Kemp, T. J., 1994. Quantum Chemical and Statistical Theory of Solutions: A computational Approach. Ellis Horwood, London, 1653-1661.

Song, M., Luo, C., Li, F., Jiang, L., Wang, Y., Zhang, D., *et al*., 2015. Anaerobic degradation of Polychlorinated Biphenyls (PCBs) and Polychlorinated Biphenyls Ethers (PBDEs), and microbial community dynamics of electronic waste-contaminated soil. *Science of the Total Environment*, **502**: 426-433.

Tokarz, I. J. A., Ahn, M. Y., Leng, J., Filley, T. R., and Nies, L., 2008. Reductive debromination of polybrominated diphenyl ethers in anaerobic sediment and a biomimetic system. *Environmental Science & Technology*, **42** (4): 1157-1164.

Wang, R., Tang, T., Lu, G., Huang, K., Chen, M., Tao, X., *et al*., 2017. Formation and degradation of polybrominated dibenzofurans (PBDFs) in the UV photolysis of polybrominated diphenyl ethers (PBDEs) in various solutions. *Chemical Engineering Journal*, **337**: 333-341.

Wang, Y. F., Wu, Y., Pi, N., and Tam, N. F., 2014. Investigation of microbial community structure in constructed mangrove microcosms receiving wastewater-borne Polycyclic Aromatic Hydrocarbons (PAHs) and Polybrominated Diphenyl Ethers (PBDEs). *Environmental Pollution*, **187**: 136-144.

Xu, X., Wang, X. D., Li, X. G., and Liu, Q. Z., 2021. A theoretical study on the photodegradation mechanism of the endocrine disrupting chemical p-nonylphenol induced by •OH in water. *Marine Pollution Bulletin*, **173** (Part B): 113107.

Zhao, C. H., Yan, M., Zhong, H., Liu, Z. F., and Shi, L. S., 2018. Biodegradation of polybrominated diphenyl ethers and strategies for acceleration: A review. *International Biodeterioration and Biodegradation*, **129**: 23-32.

Zhu, B. Q., Shi, W., and Hu, G. J., 2017. The pollution status and research progress on halogenated flame retardants in China marine environment. *Environmental Chemistry*, **36** (11): 2408-2423.

(Edited by Ji Dechun)